Lane, A. L.., Peterson, P. G., Hedley, C. B., McColl, S. T., & Fuller, I. C., 2016. Using ground penetrating radar to map soil drainage patterns to improve irrigation efficiency. In: *Integrated nutrient and water management for sustainable farming*. (Eds L.D. Currie and R.Singh). http://flrc.massey.ac.nz/publications.html. Occasional Report No. 29. Fertilizer and Lime Research Centre, Massey University, Palmerston North, New Zealand. 10 pages.

MAPPING OF ALLUVIAL SUB-SURFACE FEATURES USING GROUND PENETRATING RADAR TO IMPROVE IRRIGATION EFFICIENCY

A.L. Lane [1], P.G. Peterson [2], C.B. Hedley [2], S.T. McColl [1], I.C. Fuller [1]

[1] Institute of Agriculture and Environment, Massey University, Palmerston North 4442, New Zealand
[2] Landcare Research Limited, Palmerston North 4442, New Zealand
Email: angelalane.nz@gmail.com

Abstract

Soil drainage information is vital for determining smart irrigation practices. Predicting soil drainage requires knowledge of the spatially varying subsurface features, e.g. soil-thickness, flow pathways, and depth to groundwater table. Obtaining information about these features rapidly and non-invasively requires the use of geophysical techniques like ground penetrating radar (GPR). While applications of GPR are diverse, ranging from geotechnical to archaeological investigations, to mineral and groundwater exploration, GPR has not been extensively applied in soil mapping for agricultural purposes. The potential use of GPR for identifying subsurface features, such as depth to gravel and groundwater table which influence soil drainage, could benefit future developments in irrigation practice. To assess applicability of GPR for this purpose, research work was conducted on the alluvial soils at Massey No. 1 Dairy Farm, Palmerston North. Radargrams were collected on two 0.4 ha plots, one arable and one pasture using 200 MHz antennae, in a 2-m grid pattern. Radargrams were ground-truthed with 13 soil cores and 21 auger holes, targeting different layers detected by GPR. The soil cores were analysed for bulk density, soil moisture and particle size. Several transect lines using a 100 MHz antenna were also conducted in the pasture plot to determine soil layering and subsurface features at greater depths than what was achieved with the 200 MHz antenna. The soil types present at these sites are the Manawatu silt loam over sand, Manawatu fine sandy loam, and the Rangitikei silt loam, which overlay Manawatu River gravels that occur at depths ranging from 0.7-3 metres. Initial validation of radargrams with soil core samples indicates that GPR can obtain meaningful results from alluvial sediments ranging from sandy loams to silt loams. The use of GPR for delineating sub-surface features in alluvial soils is a promising tool that could assist with informing irrigation practice.

Introduction

Predicting soil drainage is vital if new precision irrigation technologies are to be utilised effectively. This requires an understanding of soil physical features, from the surface through the vadose zone, to groundwater. Identifying physical features that attribute to soil drainage has previously been time consuming and labour intensive e.g. pit excavations, installation of piezometers and observation wells. Ground penetrating radar, a geophysical tool provides an avenue whereby the physical features of depth to gravel, groundwater and soil horizon formation can be detected rapidly and non-invasively (Adamchuk et al., 2004). Predicting

drainage requires knowledge of the spatially varying subsurface features of the soil, e.g. soil-thickness, flow pathways, depth to gravel and depth to groundwater table. Further to soil sub-surface physical features, Information on the spatial distribution of soil water is important for precision agriculture programs (Huisman et al., 2003). In areas of intricate and contrasting soil patterns, undulating topography, and non-homogenous materials, groundwater flow patterns are more difficult to assess. Delineating these features with the assistance of GPR could effectively result in improved irrigation and farming practices, hereby minimising the loss of water and nutrients. In addition to identifying groundwater, it is important to identify other features that control water movement. Harari, (1996), identified that the internal bedding patterns can affect the flow of fluids. The ability to map these features to predict soil drainage patterns rapidly and non-invasively would make soil subsurface assessments more affordable and less damaging to the soil itself.

Ground penetrating radar uses a transmitter and receiver antennae to transfer short pulses of high-frequency (MHz to GHz) electromagnetic waves through the sub-surface (Davis & Annan, 1989). These electromagnetic waves take measurements as a function of time. The electrical properties of geological materials are primarily controlled by the water content (Davis & Annan, 1989). Variations to these electrical properties results in these waves penetrating through the sub-surface at differing velocities. This change in velocity results in a portion of the electromagnetic wave being reflected and a real-time image being produced of the sub-surface (Davis & Annan, 1989). The amount of energy that is reflected by an interface is depended upon the contrast in the relative dielectric permittivity of the two layers (Doolittle et al., 2006). For example, air, sand and distilled water have dielectric permittivity's of 1, 2 and 81 respectively (Harari, 1996). The electrical conductivity of subsurface materials determines how well the electromagnetic wave will penetrate through each material. The depth of penetration by GPR can be severely limited by an increase in electrical conductivity. For example, clays increase signal attenuation and prevent further penetration of GPR due to the energy lost from the polarization effect of electromagnetic energy on colloidal clay particles (Harari, 1996).

Resolution and depth penetration are both useful features of GPR (Huisman et al., 2003). Increasing resolution will minimise the depth penetrated and likewise, aiming for depth will minimise resolution. Controlling these features relies on the frequency bandwidth of the GPR and the medium that is being surveyed (Davis & Annan, 1989; Huisman et al., 2003). Low conductivity media such as dry sand and gravel, using a low frequency antenna (50 – 100 MHz) can achieve penetration up to tens of metres and high frequency antennas (e.g. 450 – 900 MHz) achieve penetration of one to several metres. Ground penetrating radar is not suited to all soil types due to attenuation properties decreasing the depth and resolution in some soils as previously described (Doolittle & Collins, 1995). We tested the application of GPR over alluvial soils where predominantly sand and some silt deposits lay.

This report will outline the application of GPR as a tool to identify soil drainage features from radargram images. Further analysis is yet to be conducted relating to soil particle size, bulk density and soil moisture. Research conducted in late February 2016, will allow comparisons of radargrams with soil moisture and groundwater levels between spring (September) 2015 and late summer (February) 2016 when soil moisture and groundwater levels were lower.

Materials and Methods

Study Site

The study area is located on the upper alluvial terraces of Massey Dairy No. 1 farm adjacent to the Manawatu River, approximately 2 km east of Palmerston North. Two 0.4 ha (40 x 100 m) study sites were used; a pasture plot (1) and an arable plot (2) (Fig 1, 2, 3 & 4). The pasture plot has the Manawatu silt loam and the Rangitikei silt loam over sand present with elevation 22 – 25 m above sea level. A distinct topographical change approximately halfway across the plot is seen on LiDAR imaging and this forms the boundary between the soil types. The arable plot has the Manawatu silt loam over sand and the Manawatu sandy loam present (24 – 27 m above sea level). Once again LiDAR imaging highlights a distinct topographical change diagonally across this site and forms the boundary between the two soil types. Fluvial processes have dominated the landscape of this area.

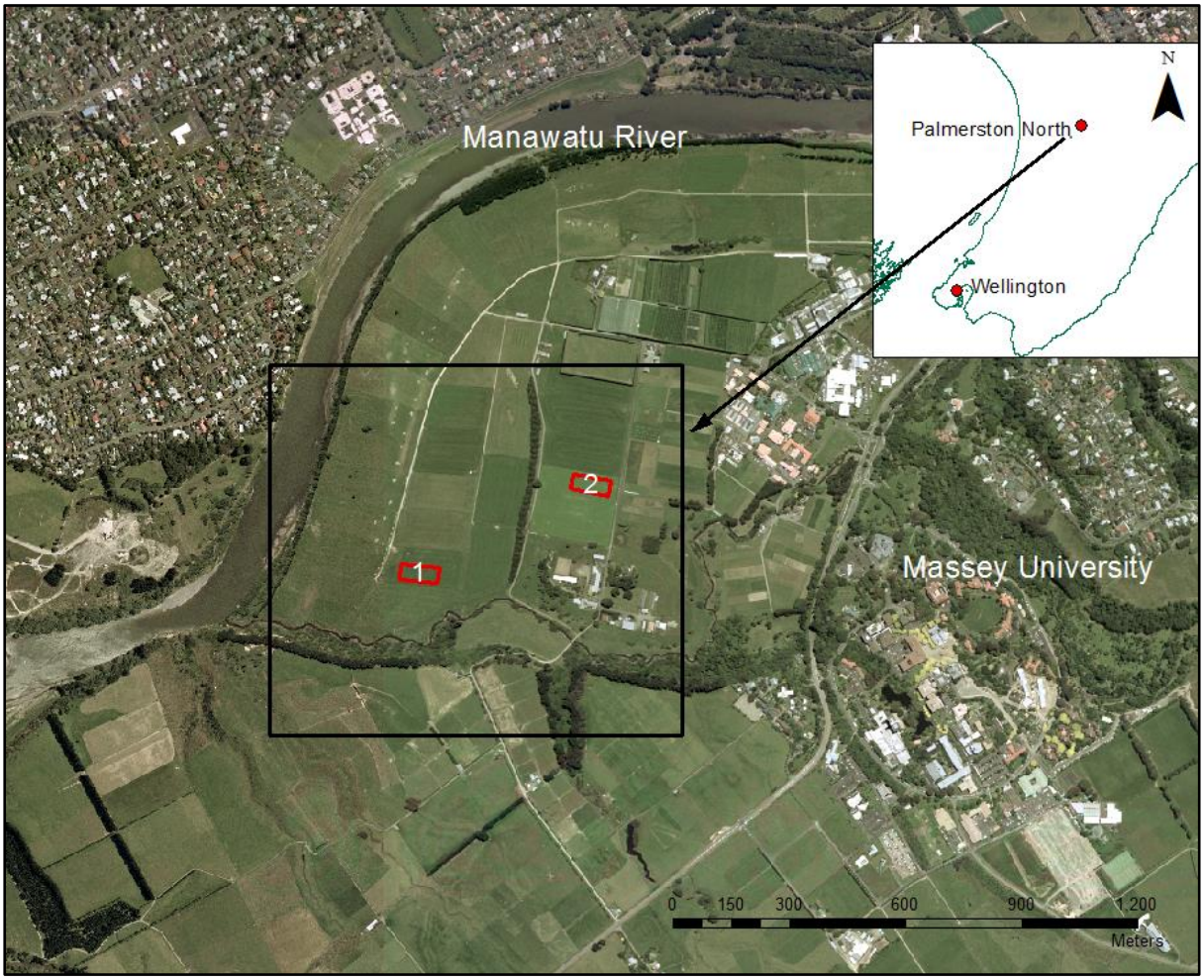

Figure 1 Location of the two 0.4 ha plots on Massey Dairy No. 1 farm, Palmerston North. Plot 1 - pasture and Plot 2 - arable

Figure 2 Pasture plot (left), arable plot (right)

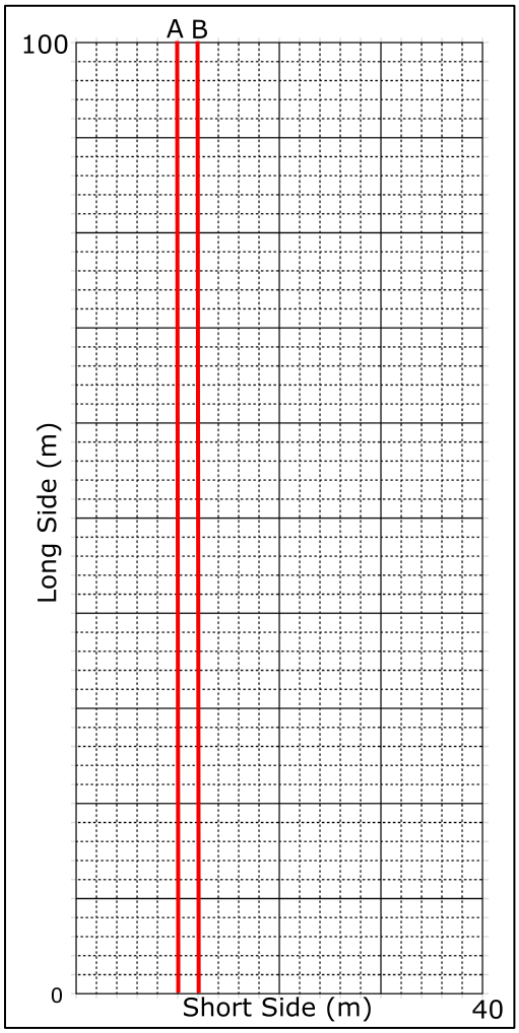

Figure 3 Diagram of the pasture plot with all 200 MHz GPR transects shown at 2 m spacings by dotted and solid black lines. GPS coordinates recorded at each solid black line intersection. 100 MHz radargram represented by transect A (10 m long line) and 200 MHz radargram represented by transect B (12 m long line) are discussed further.

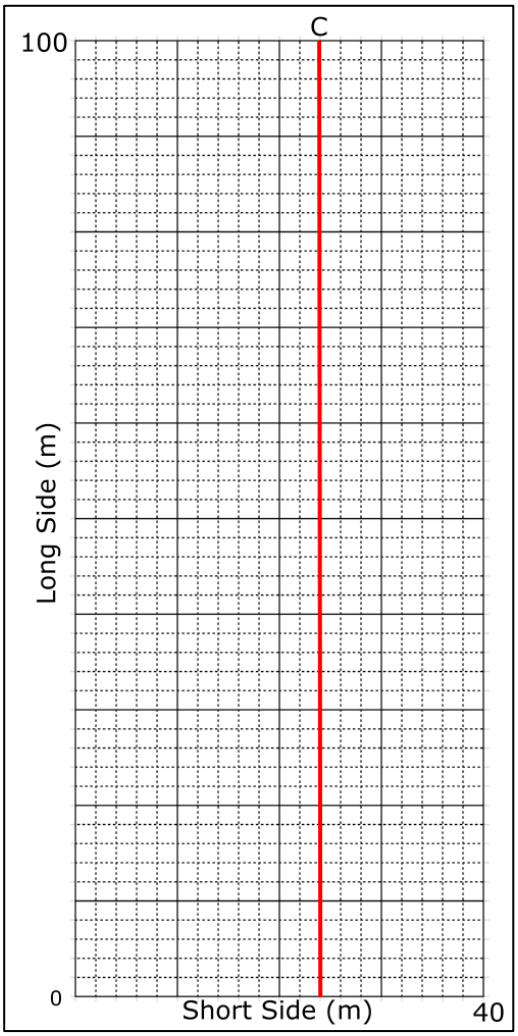

Figure 4 Diagram of the arable Plot showing all 200 MHz GPR transects at 2 m spacings, represented by dotted and solid black lines. GPS coordinates recorded at each solid black line intersection. 200 MHz radargram represented by transect C (24 m long line) and will be discussed further.

Soil Analysis

Thirteen soil cores (0.067 m diameter by depth to gravel) in and around the two sites were collected (eight cores from the pasture plot and five cores from the arable plot) using a Giddings rig corer. The locations for these were chosen after a preliminary review of the radargrams to target features of interest. This provided an avenue for ground-truthing radargrams. Cores were logged into pedological horizons based on texture and soil structure. Once soil horizons had been identified, one sample from each major horizon was analysed for bulk density, volumetric water content and particle size. A typical core profile consisted of a sandy loam or silt loam A horizon (≈ 10 cm in pasture plot and ≈ 25 cm arable plot), followed by a sandy loam B horizon with interbedded silt and sand layering in the pasture plot and generally a sandy C horizon in the arable plot. Core lengths varied depending on depth to gravel layers from 0.7 – 3 metres depth. Twenty-nine auger samples were taken across the two plots to determine depths to gravel. Initially auger samples were collected to minimise damage to the soil coring equipment.

Piezometer measurements

Four piezometers are located adjacent to the pasture plot site. This allowed for easy measurement of groundwater at the time of GPR survey. Measurements were collected prior to undertaking the 200 MHz and 100 MHz GPR surveys.

LiDAR Data

Using the geographic information system, ArcMap, a 1 meter LiDAR derived digital terrain model (DTM) and hillshade model were attained for the study site (Fig 5). This allowed interpretation of topographic features and comparison with GPR data.

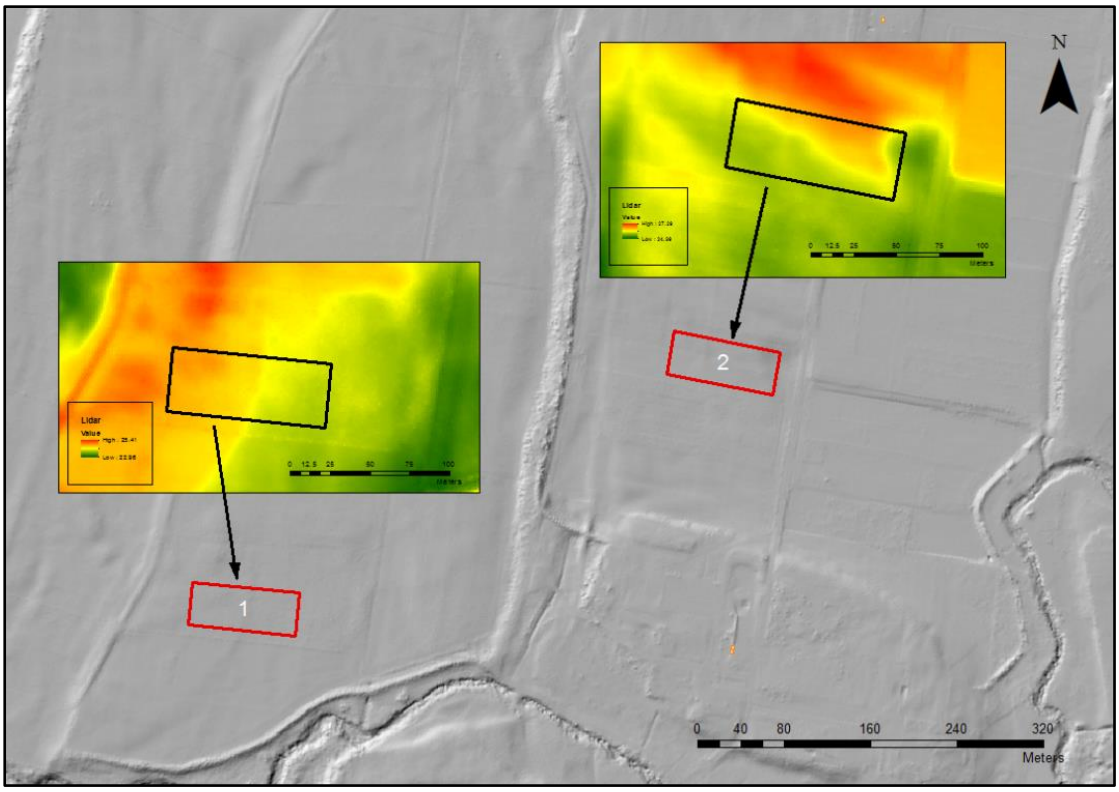

Figure 5 LiDAR and Hillshade models of the study site, showing sharp contrasts at both plots indicating former river channels

Ground Penetrating Radar Data and GPS

During September 2015 a Sensors & Software GPR system with two 200-MHz antennas was used in bi-static mode. This system was pushed across the soil surface using a PVC trolley. The 200 MHz antenna was selected as it provided good resolution to the depths of gravel. Data was acquired for both the pasture and arable plots along transects in a grid pattern that were 2 m apart to make up a total area of 0.4 ha per site (40 x 100 m). Grid coordinates were collected at 10-m intervals using a Trimble® R8 RTK-dGPS across both plots (Fig 3 & 4). To determine features at a greater depth, the 100 MHz antenna (lower frequency), was used. Two transects were acquired in the pasture plot only as access to piezometers adjacent to this plot allowed for ground-truthing radargrams.

Post Processing

Processing of radargrams was conducted using the EKKO View Deluxe, GFP Edit 4 and EKKO Project 3 software packages. All radargrams were corrected for depth using the hyperbolic velocity adjustment and rubber-banded to fit within the measured distance using EKKO View Deluxe software. Radargrams were then collated manually within the GFP Edit 4 software to form a XY grid. These included reversing directions of every second transect line to imitate data collection and altering X and Y start positions. Once grids of the two plots were established, they were then inputted into the EKKO Project 3 software for slice view imaging and interpretation of subsurface features.

Results and Discussion

Pasture Plot

Figure 6 shows the processed radargram from a transect that crossed the pasture plot at 12 m along the short side to cover the length of the plot (Fig 3, line B). The two-way travel time range is 150 ns, which corresponds to a depth range of approximately 5 metres at this site. In Fig 6, marker A defines an important internal structural feature of this radargram, a possible infilled channel. This is highlighted by the strength of cross-laminations and the obvious outline of the cross-section. The strong reflections are indicative of a change in electrical conductivity due to the interbedding of finer material (silt and clay) with sand. The finer the material, the greater the surface area for water to be held, indicating an increase in electrical conductivity. Doolittle, (2006), states that abrupt and contrasting differences in density, grain size and moisture contents will produce high amplitude reflections and this is evident within the infilled channel to the left of Fig 6 and above 2 m depth along the remainder of the image. Fig 6, marker B, shows the layer at which there is high attenuation. This zone could be interpreted as an area holding moisture (wetting front) or an area of contrasting sediments. For example, depths to gravel along this transect ranges from 2 m at the base of the infilled channel up to 0.70 m towards the right of the image. Marker B is located at approximately 2.75 m below the surface and could indicate a change from gravel to finer sediments or a possible transition zone known as a capillary fringe where partially saturated to saturated water may be present (Doolittle et al., 2006). Depth to groundwater was measured at approximately 4 m depth at the pasture plot in September 2015. However this was not clearly evident on the radargrams due to a large capillary fringe. Using a 100 MHz antenna (Fig 7) signal attenuation begins at 4 m and gradually increases to approximately 6 m depth. Finer silt loams were groundtruthed at this depth with soil cores and this correlates well with signal attenuation at this location.

Figure 8 and 9 are representations of the pasture plot at 2.21 – 2.34 m and 2.60 – 2.73 m depth below the surface respectively. Radargrams collected during September 2015 were interpolated to form a grid that could be read in slice view mode. Approximately 30 – 45 m diagonally across the plot forms the boundary of the infilled channel (Fig 8). The strong GPR reflections that have been observed to the left of Fig 8 and throughout Fig 9 are attributed to the impedance contrast provided by the change in grain size, density and soil moisture across the lamination boundaries (Doolittle et al., 2006). Figure 9 reflects that seen in Fig 6, marker B where there is a contrast between soil saturation, grain size or density at 2.60 – 2.73 m approximately below the surface.

Although the depth to groundwater has not been clearly identified in either the 100 MHz or 200 MHz radargram images due to finer sediments creating a strong capillary fringe, the ability to groundtruth with piezometer measurements at this site has given an understanding as to why the GPR signal has been attenuated.

Comparing the LiDAR image of the pasture plot (Fig 5) with Fig 8, suggests that surface topography can be reflected further down the soil profile. The same strong contrast is seen in both images suggesting GPR could be useful to identify why such changes occur at the surface i.e. the infilling of a channel and what could possibly happen with future land changes.

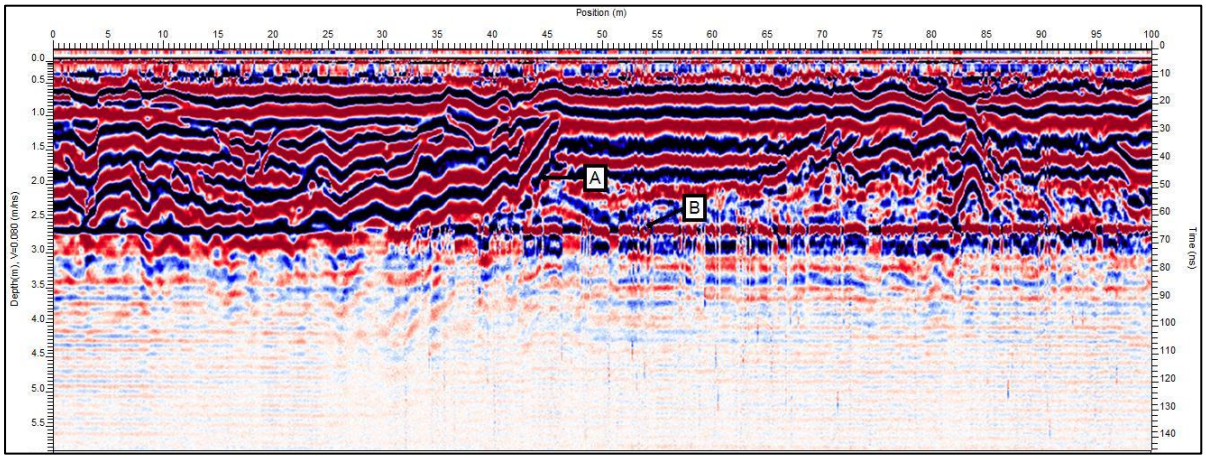

Figure 6 Radargram (using 200 MHz antenna) highlighting an infilled channel (A) and underlying deeper sediments of possible wetting front (B).

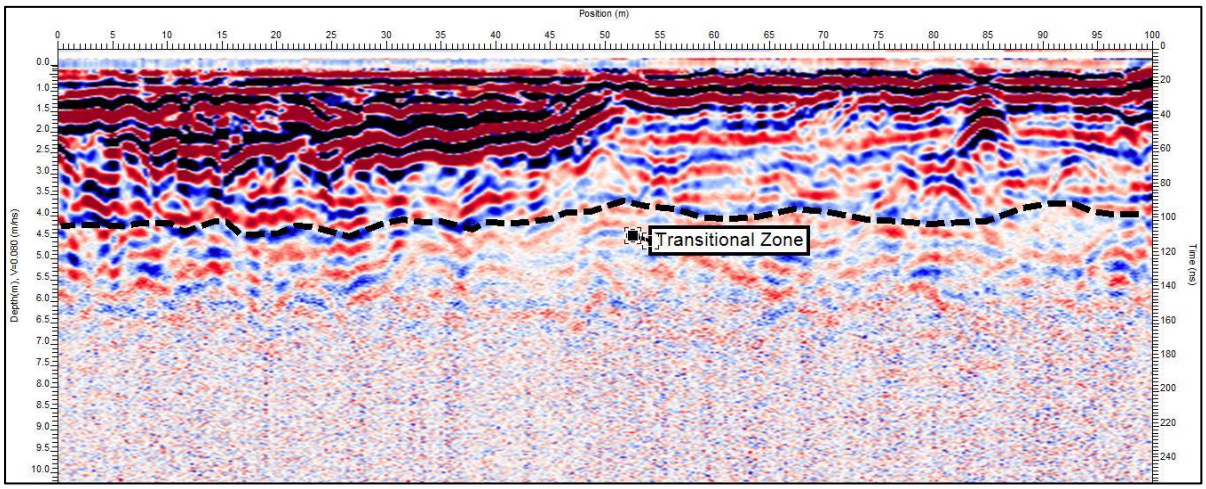

Figure 7 Radargram (using 100 MHz antenna) showing a transitional zone that occurs above the water table

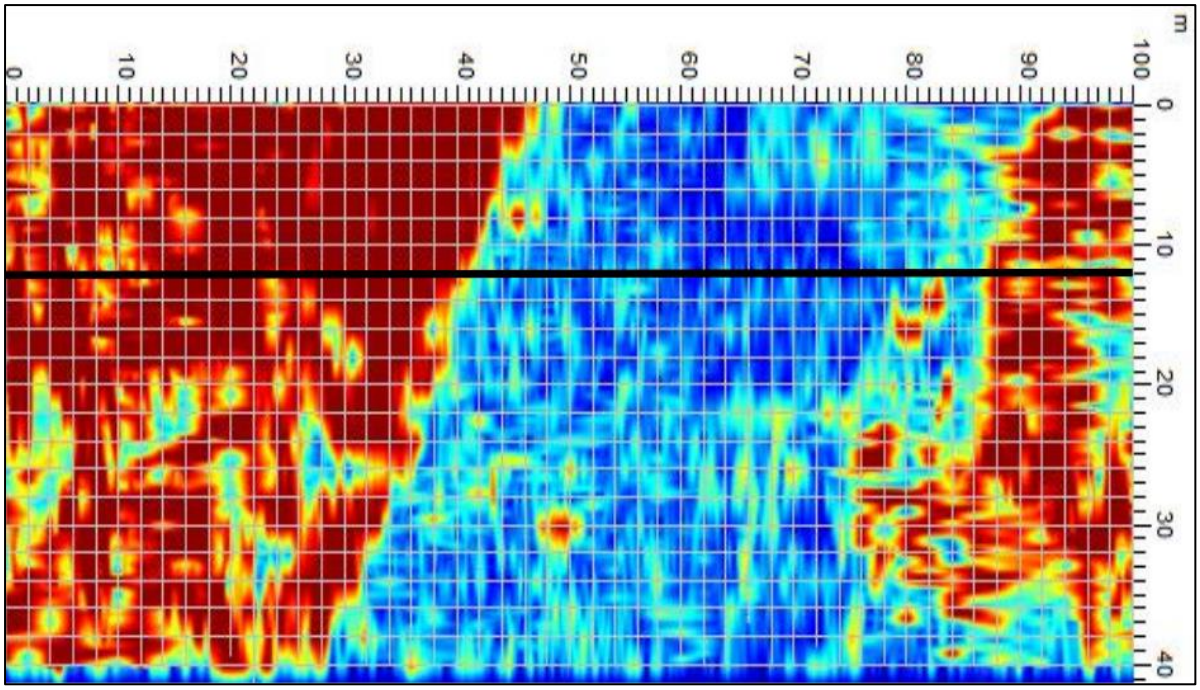

Figure 8 Slice view 2.21 – 2.34 m depth below ground. The black line indicates the 12 m long transect (Fig 3, B, Fig 6)

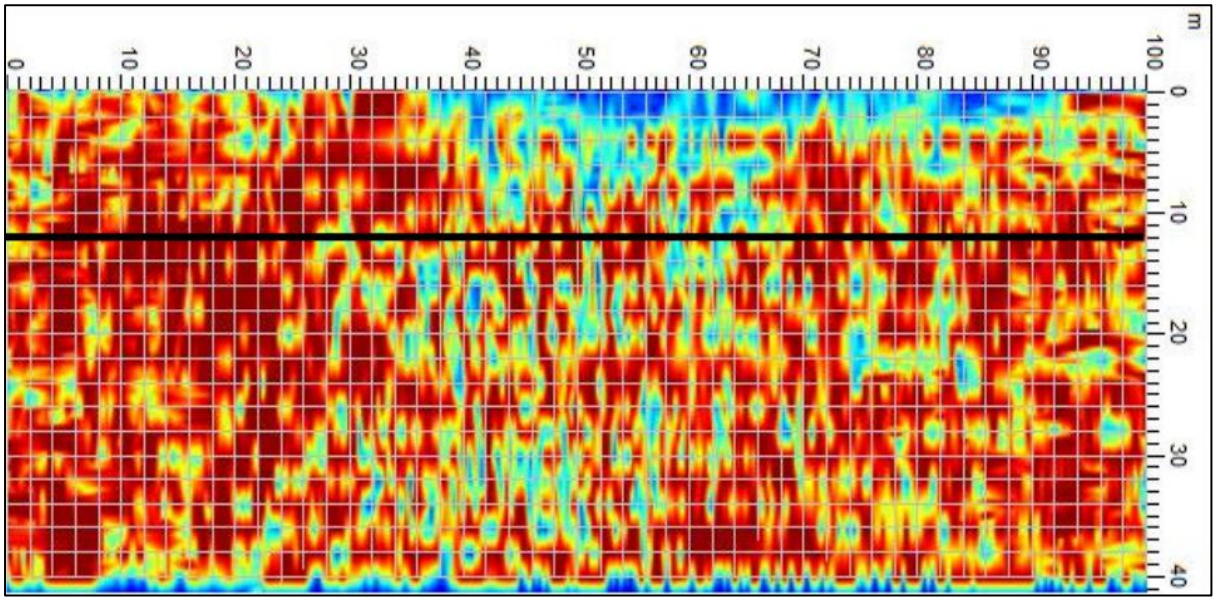

Figure 9 Depth slice view at 2.60 – 2.73 m depth below ground correlating with Fig 6, marker B where deeper finer sediments or a wetting front are located. The black line indicates the 12 m long transect (Fig 3, B)

Arable Plot

Figure 10 shows a radargram of the arable plot at the 24 m transect (Fig 4, marker C). The strong reflectors between 0.50 – 1.0 m depth are a contrast between fine and coarse sand with a possible change in soil moisture levels as groundtruthed with soil cores. This change in grain size and soil moisture is revealed by the strong reflections shown in Fig 10, marker A

and also Fig 11 across the plot (red) at 0.52 – 0.65 m depth. Further down the profile another significant change occurs at Fig 10, marker B. This is indicative of the depth to gravel as groundtruthed from auger samples. Figure 10, marker C follows a similar trend to marker B and since attenuation is strong below this point this could be indicative of groundwater. The stronger groundwater reflector shown in Fig 10, marker C compared to Fig 6, could be related to the differing soil types within these two plots. The arable plot has soil types that have a larger sand fraction at depths. This in turn creates a smaller capillary fringe therefore creating a stronger and more prominent reflection at the lamination boundary.

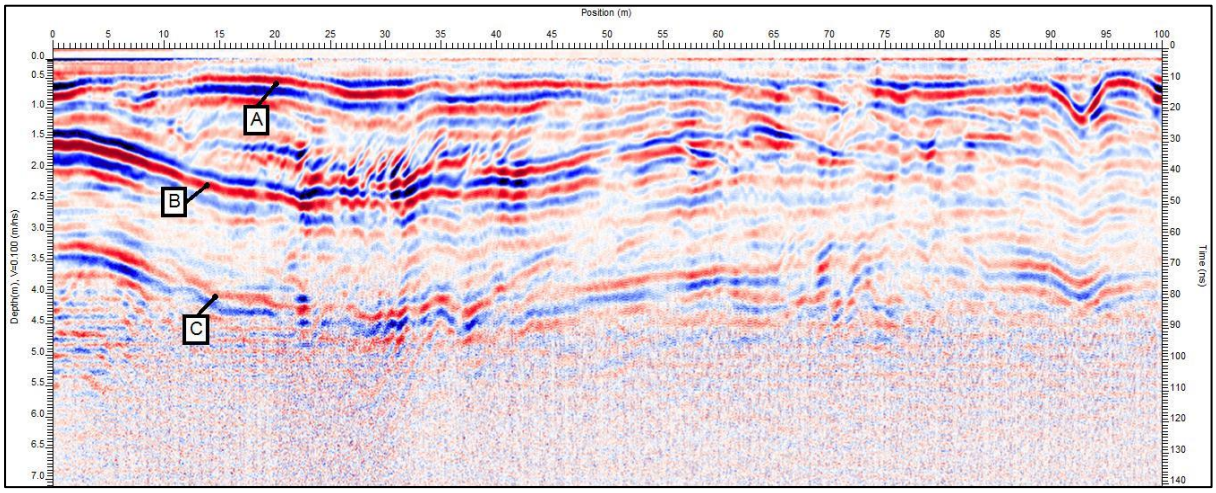

Figure 10 Radargram at the 24 m long transect (Fig 4, marker C), identifying strong GPR reflections occurring at laminar boundaries (A), depth to gravel (B); possible water table (C).

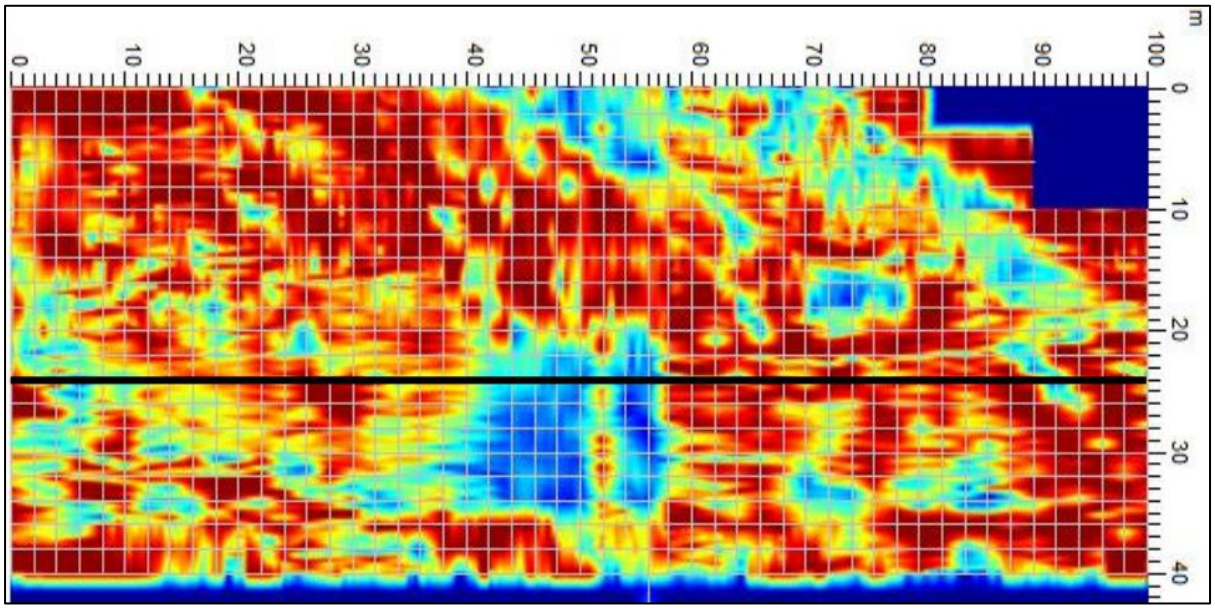

Figure 11 Depth slice at 0.52 - 0.65 m below the surface of the arable plot. The black line indicates the cross-sectional image of Fig 10, (Fig 4, C). This image focuses on strong GPR reflections across the plot as shown by Fig 10, marker A, with weaker signals between 40 – 55 m along the plot.

Conclusion

Ground penetrating radar has proven to be useful for mapping some sub-surface features in recent alluvium. For example, it has allowed rapid determination of the depth to gravel below fine-grained alluvium, and potentially can image wetting fronts and the capillary fringe, the transitional zone to the groundwater table. The use of depth-slices helped with the identification and mapping of sub-surface structures, such as infilled channels, which can help with interpreting high-resolution topographic data such as that derived from LiDAR, as well as identifying features not expressed at the surface. The next step in this project is to use the radar depth slices to produce a contour map of depth-to-gravel for each plot. Beyond that, we intend to compare radargrams between the data collected in September 2015 to subsequent surveys conducted during late February 2016 when soils are expected to be drier. This will allow us to assess whether GPR can also be used to differentiate soil moisture conditions in alluvial sediment. Although attenuation is greater in soils with finer grained material, GPR can provide a means for identifying sub-surface features, which ultimately may assist with improvements to irrigation practice.

Acknowledgments

Jolanda Amoore, Dairy 1 Farm Manager for assisting with access to the piezometer paddock; John Dando, Landcare Research for collecting the soil cores and augering; Eric Breard, Massey University for assistance with laser particle analysis; Brian Aspin Scholarship, Colin Holmes Dairy Scholarship, Horizons Advanced Sustainable Land Use Scholarship and George Mason Sustainable Land Use Scholarship for assistance with funding Angela Lane's Masters study.

References

Adamchuk, V. I., Hummel, J. W., Morgan, M. T., & Upadhyaya, S. K. (2004). On-the-go soil sensors for precision agriculture. *Computers and Electronics in Agriculture, 44*(1), 71-91.

Davis, J. L., & Annan, A. P. (1989). Ground-penetrating radar for high-resolution mapping of soil and rock stratigraphy. *Geophysical Prospecting, 37*(5), 531-551.

Doolittle, J. A., & Collins, M. E. (1995). Use of soil information to determine application of ground penetrating radar. *Journal of Applied Geophysics, 33*(1–3), 101-108. doi: http://dx.doi.org/10.1016/0926-9851(95)90033-0

Doolittle, J. A., Jenkinson, B., Hopkins, D., Ulmer, M., & Tuttle, W. (2006). Hydropedological investigations with ground-penetrating radar (GPR): Estimating water-table depths and local ground-water flow pattern in areas of coarse-textured soils. *Geoderma, 131*(3–4), 317-329. doi: http://dx.doi.org/10.1016/j.geoderma.2005.03.027

Harari, Z. (1996). Ground-penetrating radar (GPR) for imaging stratigraphic features and groundwater in sand dunes. *Journal of Applied Geophysics, 36*(1), 43-52. doi: http://dx.doi.org/10.1016/S0926-9851(96)00031-6

Huisman, J. A., Hubbard, S. S., Redman, J. D., & Annan, A. P. (2003). Measuring soil water content with ground penetrating radar: A review. *Vadose Zone Journal, 2*(4), 476-491.